

**Electronic Supporting Information (ESI) for the manuscript:**

**Heptazine based organic framework as chemiresistive sensor for ammonia detection at room temperature**

Nidhi Sharma,<sup>a</sup> Neha Sharma,<sup>a</sup> Parthasarathy Srinivasan,<sup>b</sup> Sunil Kumar,<sup>a</sup> John Bosco Balaguru Rayappan,<sup>\*b</sup> and Kamalakkannan Kailasam<sup>\*a</sup>

<sup>a</sup> Institute of Nano Science and Technology, Habitat Center, Phase 10, Mohali 160062, Punjab, India. E-mail: [kamal@inst.ac.in](mailto:kamal@inst.ac.in)

<sup>b</sup> Centre for Nanotechnology & Advanced Biomaterials, School of Electrical & Electronics Engineering, SASTRA Deemed University, Thanjavur - 613 401, India

1. Reaction scheme.
2. Photograph of the overall HMP-TAPB-1 sensor platform.
3. Electrical properties of microporous polymer based sensor: I-V characteristics and Hall measurement.
4. Linear relationship between concentration and sensing response.
5. Sensitivity curve of NH<sub>3</sub> in presence of different relative humidity conditions.
6. Comparison of various ammonia gas sensors operated at room temperature.

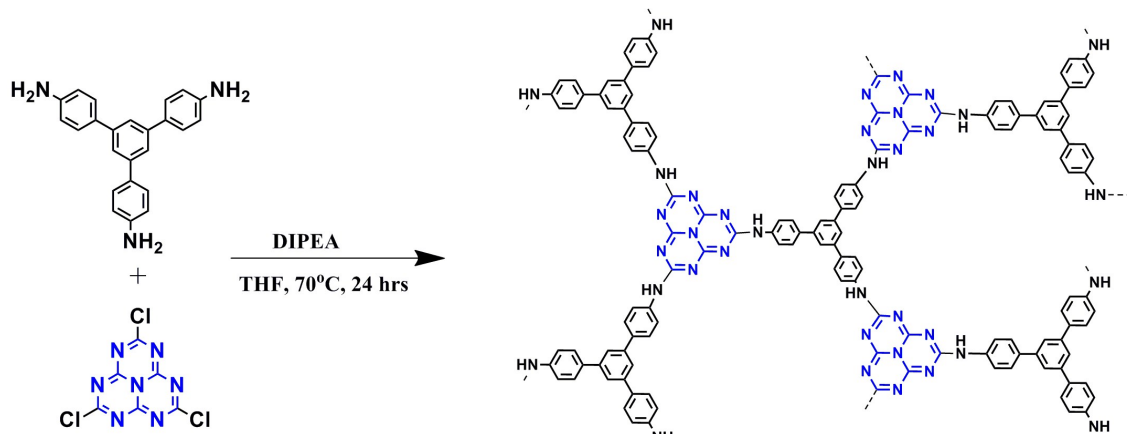


**Fig. S1.** Molecular structure of HMP-TAPB-1 and reaction scheme.

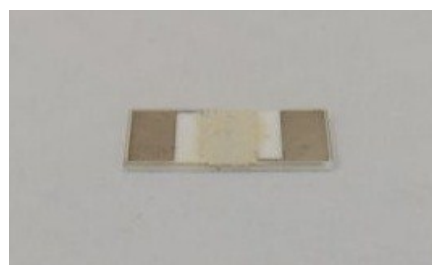


**Fig. S2.** Photograph of the overall HMP-TAPB-1 sensor platform.

**Electrical Properties of Microporous Polymer based Sensor**

I-V characteristics of the fabricated sensor (Fig.S3 (a)) showed a linear relationship between the current and applied voltage in-turn confirmed the Ohmic contact between the sensing element and electrodes. Since, grain and grain boundary resistances are the influencing parameters in deciding the gas sensing response,

impedance measurements were carried out using electrochemical impedance measurement system (CHI660E, CH Instruments, USA) with gold working electrode, platinum counter electrode and Ag/AgCl reference electrode with 0.1 M of potassium hexacyanoferrate (III) as an electrolyte and is shown in Fig. S3 (b).

Fig. S3 (b) shows the Nyquist impedance plot of HTAPB-1 sample, where the grain and grain boundary resistances were estimated from the observed semicircle trend. The observed data was fitted to the simple Randles circuit (Fig. S3 inset). The grain parameters such as  $R_g$ ,  $R_{gb}$  and  $C_{gb}$  were estimated as  $74 \Omega$ ,  $124 \Omega$  and  $6.16 \mu\text{F}$ , respectively.

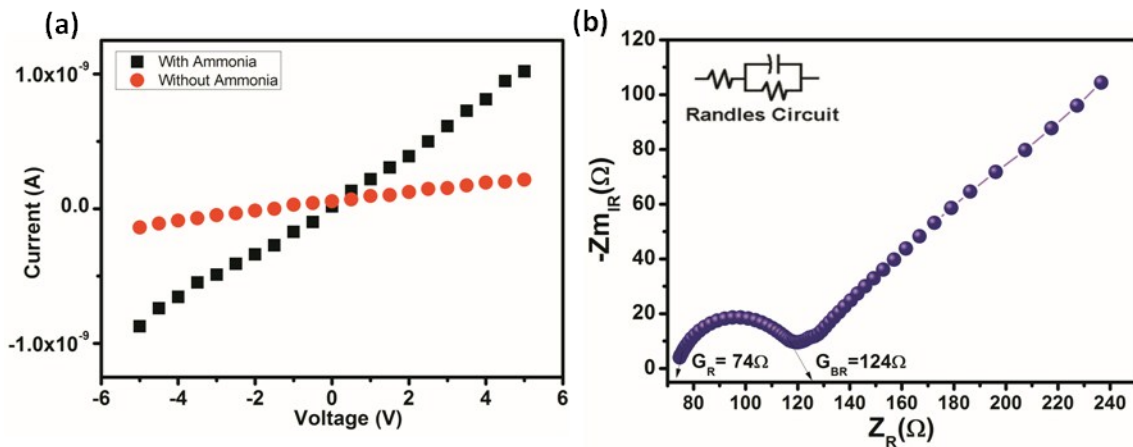


**Figure S3.** (a) I-V characteristics of the sensor and (b) Nyquist plot.

To further evaluate the electrical characteristics of the HMP-TAPB-1 sample, room temperature Hall measurement studies were carried out. The observed electrical parameters are listed in the Table S1. The negative Hall coefficient confirmed the n-type nature of HMP-TAPB-1 sample.

**Table S1.** Electrical properties of the HMP-TAPB-1 sample.

Sample	Carrier Concentration ( $\text{cm}^{-2}$ )	Mobility ( $\text{cm}^2 \text{V}^{-1}\text{s}^{-1}$ )	Resistivity	Grain Resistance ( $\Omega$ )	Grain boundary resistance ( $\Omega$ )	RHA (A-C Cross Hall Coefficient)
HMP-TAPB-1	$3.09 \times 10^{11}$	$3.16 \times 10^1$	$1.58 \times 10^7$	74	124	$-4.00 \times 10^5$

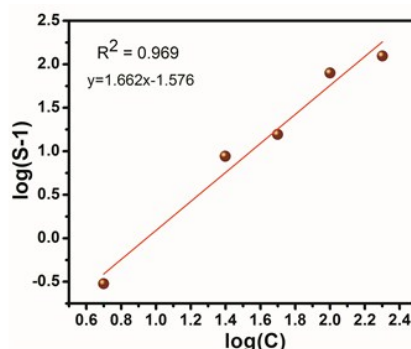


**Fig. S4.**  $\log(C)$  vs  $\log (S^{-1})$  linear fitting with goodness of fit  $R^2=0.969$  suggests the linear relationship between the concentration and sensing response

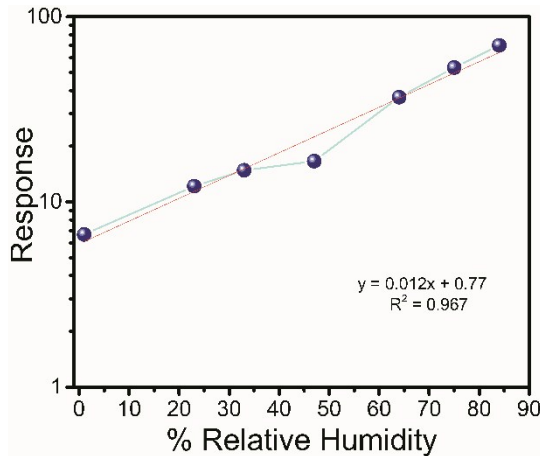


**Fig. S5.** Sensitivity curve of NH<sub>3</sub> in presence of different relative humidity conditions.

**Table S2.** Comparison of gas sensing performance of ammonia sensors operated at room temperature..

Active Material	Sensitivity	Response Time (s)	Recovery Time (s)	Operating Temp.(°C)	Selectivity (Test gases)	LOD	Influence of Humidity	Reference
PANI-nanofiber/WS <sub>2</sub> nanosheet	81% at 200ppm	260	790	RT	NH <sub>3</sub> , CH <sub>3</sub> CH <sub>2</sub> OH, CH <sub>3</sub> OH, IPA, CH <sub>3</sub> COCH <sub>3</sub> , Toluene	50ppm	Checked	<sup>1</sup>
CuCo <sub>2</sub> O <sub>4</sub> Nanoplates	7.9% at 400 ppm	120	840	RT	CO, NO <sub>2</sub> , H <sub>2</sub> S, NH <sub>3</sub>	25ppm	dry air and 47%RH	<sup>2</sup>
OMCs	~6.3 at 25ppm	120	240	RT	NH <sub>3</sub> , CH <sub>4</sub> , H <sub>2</sub> , CO <sub>2</sub> , CH <sub>3</sub> OH, C <sub>2</sub> H <sub>5</sub> OH, CH <sub>3</sub> COCH <sub>3</sub> , Benzene	1ppm	1725 ppm water vapor	<sup>3</sup>
BPB/R-GO	5.50% at 25ppm	210	-	RT	NH <sub>3</sub>	5ppm	Checked	<sup>4</sup>
Amorphous CTF	17.2% at 100ppm	100	420	RT	NH <sub>3</sub>	10ppb	-	<sup>5</sup>
PQT-12	8.6% for 100ppm	8	103	RT	NH <sub>3</sub> , Acetone, Methanol	300ppb*	Checked	<sup>6</sup>
ZnO-T-CNT networks with 2.0 wt % CNT	300 at 100ppm	18.4	35	RT	NH <sub>3</sub> , H <sub>2</sub> , Ethanol	200ppb*	30 and 75%RH	<sup>7</sup>
V <sub>2</sub> O <sub>3</sub> Nanosheet	2.4 at 25ppm	183	60	RT	NH <sub>3</sub> , Acetone, Ethanol, IPA, CH <sub>3</sub> CHO, NO <sub>2</sub> , TEA	10ppm	-	<sup>8</sup>
PbSQDs/TiO <sub>2</sub> NTARs	17.49 at 100ppm	-	-	RT	NH <sub>3</sub> , Methanol, Ethanol, Acetone, Toluene	2ppm	-	<sup>9</sup>
MoSe <sub>2</sub>	12 at 500 ppm	-	540	RT	NH <sub>3</sub>	50ppm	-	<sup>10</sup>
GG/Au nanocomposite	2600% at 25 ppm	200	180	RT	NH <sub>3</sub> , CH <sub>3</sub> COCH <sub>3</sub> , CH <sub>3</sub> CN, C <sub>6</sub> H <sub>12</sub> , (C <sub>2</sub> H <sub>5</sub> ) <sub>2</sub> , CH <sub>3</sub> CH <sub>2</sub> OH, IPA, CH <sub>3</sub> OH, n-Butyl Acetate, THF, Xylene	0.1 ppb*	Checked	<sup>11</sup>
2D SnS <sub>2</sub>	4.2 at 500ppm	16	450	RT	NH <sub>3</sub> , Ethanol, CO, Benzene, H <sub>2</sub> S, H <sub>2</sub> , NO <sub>2</sub> , CH <sub>3</sub> CHO	20ppm	(40,60 and 80) %RH	<sup>12</sup>
HMP-TAPB-1	16.6(@47%RH) 70(@84%RH) at 50ppm	65	9	RT	NH <sub>3</sub> , CH <sub>3</sub> COCH <sub>3</sub> , CH <sub>3</sub> CH <sub>2</sub> OH, HCHO, CH <sub>3</sub> CHO, Benzene, Toluene, TEA, TMA, IPA, Acetylacetone, NO <sub>2</sub>	1ppm	(23-84) %RH	<b>Present work</b>

Note: Sensitivity; S= R<sub>a</sub>/R<sub>g</sub> or ΔR/R\*100% \*: Represents calculated detection limit

1. R. K. Jha, M. Wan, C. Jacob and P. K. Guha, *New Journal of Chemistry*, 2018, **42**, 735-745.
2. S. Jain, A. Patrike, S. S. Badadhe, M. Bhardwaj and S. Ogale, *ACS Omega*, 2018, **3**, 1977-1982.
3. W. Luo, T. Zhao, Y. Li, J. Wei, P. Xu, X. Li, Y. Wang, W. Zhang, A. A. Elzatahry, A. Alghamdi, Y. Deng, L. Wang, W. Jiang, Y. Liu, B. Kong and D. Zhao, *Journal of the American Chemical Society*, 2016, **138**, 12586-12595.
4. D. L. Thai, T. T. Quang, D. V. Quang, H. Byeong-Ung, S. Saqib, S. Il-Yung, Y. S. Kyun, C. D. June and L. Nae-Eung, *Advanced Functional Materials*, 2016, **26**, 4329-4338.
5. L.-M. Tao, F. Niu, D. Zhang, T.-M. Wang and Q.-H. Wang, *New Journal of Chemistry*, 2014, **38**, 2774.
6. C. Kumar, G. Rawat, H. Bhatt, Y. Kumar, R. Prakash and S. Jit, *Sens. Actuators, B*, 2017, **255**, 203-209.
7. F. Schutt, V. Postica, R. Adelung and O. Lupan, *ACS applied materials & interfaces*, 2017, **9**, 23107-23118.
8. V. Mounasamy, G. K. Mani, D. Ponnusamy, K. Tsuchiya, A. K. Prasad and S. Madanagurusamy, *Journal of Materials Chemistry A*, 2018, **6**, 6402-6413.
9. Y. Liu, L. Wang, H. Wang, M. Xiong, T. Yang and G. S. Zakharova, *Sensors and Actuators B: Chemical*, 2016, **236**, 529-536.
10. D. J. Late, T. Doneux and M. Bougouma, *Applied Physics Letters*, 2014, **105**, 233103.
11. S. Pandey and K. K. Nanda, *ACS Sensors*, 2015, **1**, 55-62.
12. Z. Qin, K. Xu, H. Yue, H. Wang, J. Zhang, C. Ouyang, C. Xie and D. Zeng, *Sensors and Actuators B: Chemical*, 2018, **262**, 771-779.